Monodisperse model suitable to study the glass transition

M. Pica Ciamarra, M. Tarzia, A. de Candia, and A. Coniglio
Dipartimento di Scienze Fisiche, Università di Napoli "Federico II" and INFM, Unità di Napoli, Complesso Universitario di Monte Sant'Angelo, Via Cintia, I-80126 Napoli, Italy

(Received 6 August 2003; published 23 December 2003)

We study the properties of a monodisperse lattice glass model with a simple geometrical interpretation, which reproduces many features of glass forming liquids, such as the cage effect, vanishing diffusivity, and the presence of two time scales in relaxation functions. The model has a crystalline ground state at high density, but has no tendency to crystallize when quenched, even at extremely low cooling rates, which makes it suitable for the study of the glass transition. We study the model in mean field on random regular graphs, finding a scenario analogous to *p*-spin models.

DOI: 10.1103/PhysRevE.68.066111 PACS number(s): 05.50.+q, 61.43.Fs, 05.20.−y

I. INTRODUCTION

When a liquid is cooled below the melting temperature avoiding crystallization, it enters a supercooled state. If the temperature is further decreased the liquid falls out of equilibrium and becomes a glass. As the system approaches the glassy state the motion of the molecules is slowed down, the structural relaxation time quickly changes by several orders of magnitude, and the system appears as a disordered solid on the time scale of experimental observations [1].

Several efforts have been put forward in order to understand the dynamics and thermodynamics of supercooled liquids, and the glass transition. There are many valuable theories based on free volume [2], cooperative rearrangements of particles [3], inherent structures approach [4,5], mode coupling theory [6], and replica method [7].

In the supercooled state the dynamics is dominated by the ''cage effect'': every particle is trapped in the cage formed by the surrounding particles for a long time before escaping. The above mentioned mode coupling theory (MCT) gives a quantitative description of the relaxation process of supercooled liquids. The MCT predicts the existence of a temperature T_c at which there is a dynamical arrest that arises from the nonlinear interaction of density fluctuations. The relaxation time and the inverse diffusivity diverge as a power law when T approaches T_c. The hypothesis that the glass transition is the signature of a kinetically avoided static thermodynamic transition (the ''ideal glass transition'') that would take place at a temperature $T_s<T_g$ is still under investigation. This scenario is now object of growing attention, because of the analogy with the *p*-spin glass [8], a mean field model with *p*-body interactions and quenched disorder, which reproduces many features of glass forming liquids and has a static replica symmetry breaking transition.

Because the *p*-spin glass is physically so different from a structural glass, in the Past years there have been different attempts to devise a model for the glass transition physically more appealing. In this line of research, Biroli and Mézard have introduced a lattice glass model [9] that shows in three dimensions, by means of numerical simulations, a behavior typical of glass forming liquids. Moreover the mean field solution on a random graph shows a scenario analogous to *p*-spin models, with one step replica symmetry breaking. The model is constituted by lattice glass variables $n_i=0,1$ on a lattice that interact via a *p*-body potential, with $3\leqslant p\leqslant z+1$, where z is the coordination number of the lattice, with the nearest neighbors. In order to reduce the tendency to crystallize, the authors considered a mixture of two types of particles. The model has been further studied in [10].

In this paper we consider a three-dimensional lattice gas model with a simple geometrical interpretation [11] and two-body interactions. Since the model has no tendency to crystallize, clear results on the high-density region are obtained without the introduction of a mixture. Monte Carlo simulations show that the model reproduces the behavior of glass forming liquids, and that its dynamics compare well, in many respects, with the predictions of MCT. Particularly, the correlation function of the density fluctuations displays two step relaxation, and can be fitted in the intermediate and long time regimes by the functional forms predicted by MCT. The analytical solution of the model in mean field, on a random regular graph, shows again a scenario analogous to *p*-spin models, with a 1-step replica symmetry breaking transition.

In Sec. II we introduce the model. In Sec. III we present Monte Carlo simulations and compare the dynamical behavior of the model with the predictions of MCT. The mean field analysis is presented in Sec. IV, while some conclusions are drawn in Sec. V. The Appendix gives details about the mean field calculations.

II. MODEL

The model is defined as follows. We partition the space in regular cells, such that not more that one particle can have its center of mass inside the cell. A coarse grained discrete internal degree of freedom, which can assume a finite number q of states, describes the position and the orientation of a particle inside the cell. The interaction between nearest neighbors depends explicitly on the internal degree of freedom. The model is therefore described by the following Hamiltonian

$$\mathcal{H}=\sum_{\langle ij\rangle} n_i n_j \phi_{ij}(\sigma_i,\sigma_j)-\mu\sum_i n_i, \tag{1}$$

where $n_i=0,1$ whether the ith cell is occupied by a particle or not, $\sigma_i=1,\ldots,q$ represents the internal position of the

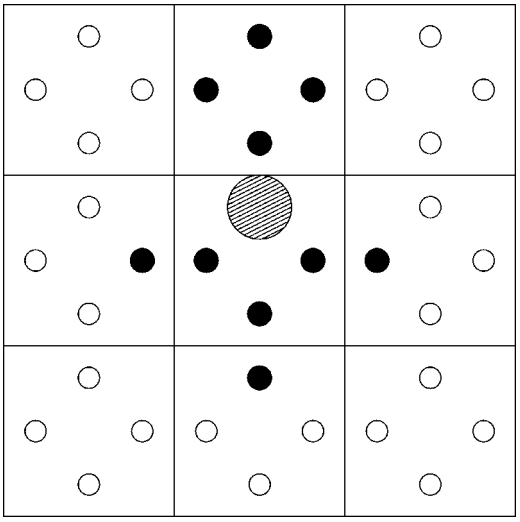

FIG. 1. The model in two dimensions: the space is partitioned in square cells, and each cells can be occupied by at most one particle in one of four positions (little circles). A particle in a given position (big shaded circle) forbids the presence of another particle in the positions colored in black.

particle, and $\phi_{ij}(\sigma_i,\sigma_j)$ is the interaction energy between two particles in cells i and j, with internal positions σ_i and σ_j, and μ is the chemical potential.

Is it clear that, by choosing a sufficiently large number q of internal positions, and an opportune interaction matrix $\phi_{ij}(\sigma_i,\sigma_j)$, one can approximate as closely as desired any model defined in the continuum, as, for example, a Lennard-Jones liquid. On the other and, it is plausible that a few number of internal states may be enough to catch the fundamental characteristics of dynamics and thermodynamics of glass forming liquids.

Here, we study a particularly simple realization of the model described by Eq. (1). In two dimensions, we partition the space in square cells, and subdivide each cell into four internal positions. When a cell is occupied by a particle in a given position, a hard-core repulsion forbids the presence of another particle in some of the internal states of the neighboring cells (see Fig. 1). Therefore in this case $q=4$, and the interaction $\phi_{ij}(\sigma_i,\sigma_j)$ is zero if the positions σ_i and σ_j are ''compatible,'' infinite otherwise. This choice can be interpreted as a coarse grained version of a hard sphere system. In three dimensions, one partitions the space into cubic cells, and considers six internal positions instead of four.

For every spatial dimension d, the model has a crystalline ground state on lattices with sides multiples of $2d+1$ lattice spacings, with density $2d/(2d+1)$, where density means fraction of occupied cells. For example, on a cubic lattice with periodic boundary conditions, the ground state can be found as follows: consider the cell with coordinates (x,y,z), and evaluate the number $a=(x+2y+3z \bmod 7)$: if $a=0$ leave the cell empty; if $a=1,2,3$ put a particle in the negative x, y, or z direction, respectively; if $a=4,5,6$ put a particle in the positive z, y, or x direction, respectively. In Fig. 2 it is shown the ground state of a two-dimensional 5×5 lattice, with density 4/5.

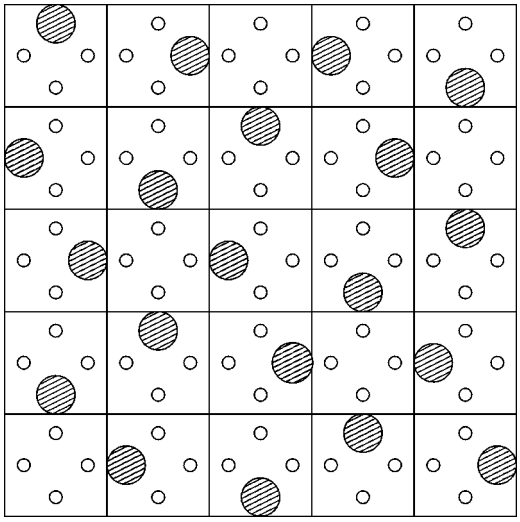

FIG. 2. Ground state of a two-dimensional 5×5 lattice, with density 4/5.

III. SIMULATIONS

We have simulated the system in three dimensions, by means of Monte Carlo canonical (fixed density) and grand-canonical (variable density) dynamics. The grand-canonical dynamics is given by the following algorithm.

(1) Pick up a site at random. If the site is occupied by a particle, then: (a) Pick up a site at random between the six nearest neighbor ones and the one occupied by the particle; (b) Choose a random internal state; (c) If doing so particles do not overlap, move the particle in the new site with the new internal state.

Otherwise, do nothing.

(2) Pick up a site at random. If the site is occupied by a particle, destroy the particle with probability $\exp(-\mu/T)$. If the site is empty, choose a random internal state and, if doing so particles do not overlap, create a new particle with the chosen internal state.

(3) Advance the time by $1/N$, where N is the number of sites.

In the canonical dynamics step 2 is missing.

The nice feature of this model is that it has no tendency to crystallize. A compression experiment on a system of size 28^3 is shown in Fig. 3. A grand-canonical dynamics is performed, and temperature is slowly decreased, starting from some high value. The results are shown as open circles in Fig. 3 for various cooling rates.

The final high-density state is strongly dependent from the cooling rate, as observed in glass forming liquids. On the other hand, no tendency to crystallization is observed, even at the slowest cooling rate ($\dot{T}/T=-10^{-7}$) no transition to the crystalline state is observed. We have also prepared the system in the crystalline states at very low temperature, and heated it up slowly (diamonds in Fig. 3). The ordered state becomes unstable at $T\simeq0.150\mu$, where the system falls into the liquid phase.

To avoid crystallization most continuum and discrete simulations of glass forming liquids consider mixtures of particles with different properties (or introduce in the Hamil-

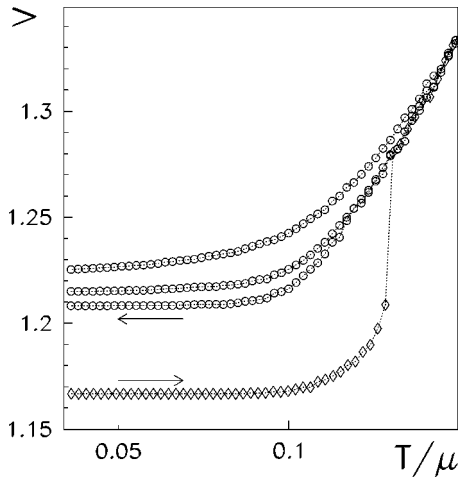

FIG. 3. Specific volume (inverse density) as a function of temperature, for a three-dimensional system of size 28^3. Circles: the system is cooled starting from high temperature for cooling rates (from top to bottom) $\dot{T}/T=-10^{-4},-10^{-5},-10^{-7}$. Diamonds: the system is heated starting from the crystalline ground state, with heating rate $\dot{T}/T=10^{7}$.

tonian some *ad hoc* terms [12]). This makes the models more complicated, and introduces in the relaxation processes two time scales that entangle with those associated with the cage effect. This is why the absence of crystallization makes this model suitable for the study of the glass transition.

After having equilibrated the system at a certain density, we switch to canonical dynamics. These simulations are performed on lattices of size 15^3. The mean square displacement of the particles is shown in Fig. 4. This is defined taking into account also the position of a particle inside a cell giving to each internal position a shift of 1/4 of a lattice spacing with respect to the center of the cell. In Fig. 5 we plot the self-overlap, defined as

$$\langle q(t)\rangle=\frac{1}{N}\sum_i \langle n_i(t'+t)n_i(t')\boldsymbol{\sigma}_i(t'+t)\cdot\boldsymbol{\sigma}_i(t')\rangle, \quad (2)$$

where the average $\langle\cdots\rangle$ is done over the time t', and $\boldsymbol{\sigma}_i(t)$ are unit length vectors, pointing in one of the six coordinates directions, representing the position of the particles inside the cell. The dynamical nonlinear susceptibility associated with the self-overlap parameter, which is defined as

$$\chi(t)=N[\langle q(t)^2\rangle-\langle q(t)\rangle^2], \quad (3)$$

is shown in Fig. 6. The susceptibility displays a maximum $\chi(t^*)$ at time t^*. The growth of $\chi(t^*)$ with the density implies that the dynamics becomes more heterogeneous at higher density. We are able to fit $\chi(t^*)$ as a function of density with a power law $(\rho_c'-\rho)^{-\gamma'}$, in which $\rho_c'=0.839$ and $\gamma'=1.9$ (inset of Fig. 6).

We have studied the self-part of the autocorrelation function of the density fluctuations, defined as

$$S_{\mathbf{k}}(t)=\frac{1}{N}\left\langle \sum_i e^{i\mathbf{k}\cdot[\mathbf{r}_i(t'+t)-\mathbf{r}_i(t')]}\right\rangle, \quad (4)$$

where $\mathbf{r}_i(t)$ is the position of the ith particle in units of lattice constants, considering as before the internal positions as shifted of 1/4 of a lattice spacing with respect to the center of the cell. Due to the discreteness and periodicity of the lattice, the wave vector must have the form $\mathbf{k}=(2\pi/L)(n_x,n_y,n_z)$, where n_x, n_y, and n_z are integers between 0 and $L/2$. We have chosen wave vector $\mathbf{k}=(\pi,0,0)$, which corresponds to a wavelength equal to two lattice spacings, because for that $\mathbf{k}$ density fluctuations $\langle|\rho_{\mathbf{k}}(t')|^2\rangle$ are largest, where $\rho_{\mathbf{k}}(t')$ is the Fourier transform

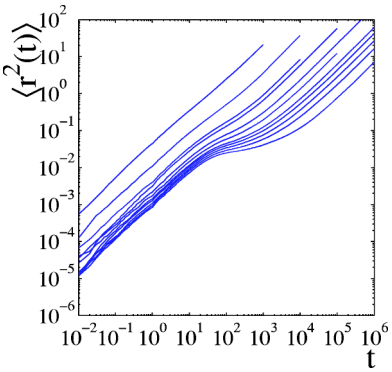

FIG. 4. Mean square displacement $\langle r^2(t)\rangle$ in a three-dimensional system of size 15^3 for densities $\rho=0.6$, 0.7, 0.75, 0.76, 0.78, 0.79, 0.8, 0.805, 0.81, 0.815, 0.82.

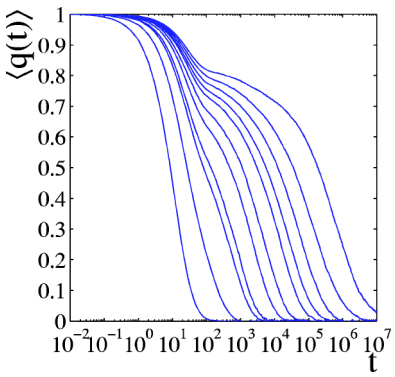

FIG. 5. Self-overlap $\langle q(t)\rangle$ as a function of time for the same density of Fig. 4.

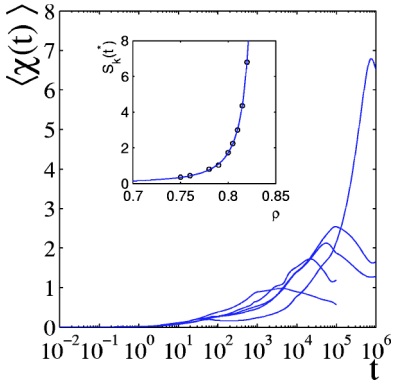

FIG. 6. Nonlinear susceptibility for density 0.78, 0.80, 0.805, 0.810, 0.820. Inset: the maximum $\chi(t^*)$ as a function of density. The fitting function is a power law $\chi(t^*)=0.003(0.839-\rho)^{-1.9}$.

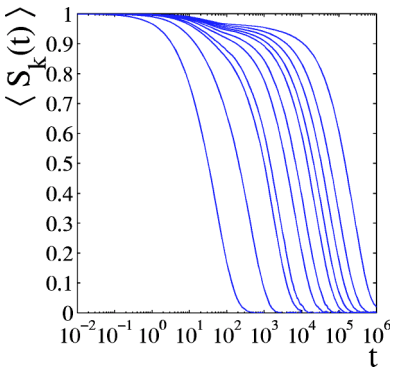

FIG. 7. Relaxation functions for the self-part of the density-density fluctuations for $\mathbf{k}=(\pi,0,0)$ and the same densities of Fig. 4.

of the density. This means that this mode is the most important in the dynamics of the system. The results for various densities are plotted in Fig. 7.

The mean square displacement, the relaxation of the density-density fluctuations, and the relaxation of the overlap show that the model reproduces the cage effect and the presence of two characteristic time scales in the relaxation process. The first one is associated to the vibration of a particle inside the cage formed by the surrounding particles, and gives rise to the first decay of the relaxation functions. The second time scale is associated to the global relaxation of the system, and gives rise to the final decay of the correlation functions.

We have then studied the behavior of the diffusion coefficient and of the inverse relaxation time (Fig. 8). They vanish at the same density $\rho_c=0.844$, with power laws $(\rho_c-\rho)^\gamma$ with the same exponent $\gamma=3.53$. The critical density ρ_c is compatible, within errors, with the density ρ_c' at which the dynamical nonlinear susceptibility diverges.

Comparison with Mode Coupling Theory

We have compared the relaxation functions of the model with the predictions of MCT. The theory predicts that, near the transition, the intermediate time behavior ($t_0 \ll t \ll t_\alpha$, with the microscopic time t_0 and the relaxation time t_α) of the relaxation functions can be fitted by

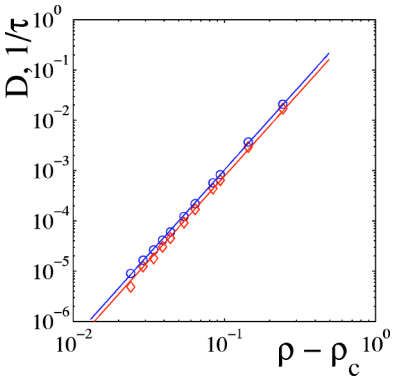

FIG. 8. Diffusion coefficient D (circle) and inverse relaxation time $1/\tau$ (diamonds) as a function of $\rho-\rho_c$. The values of the densities are the same used in Fig. 4, while $\rho_c=0.844$. The straight lines are power laws $\propto(\rho-\rho_c)^\gamma$ with $\gamma=3.53$.

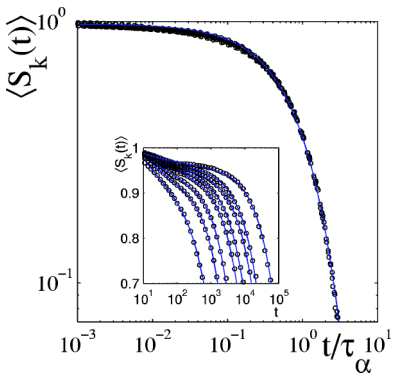

FIG. 9. Time-density superposition principle for the correlation function, for densities ρ = 0.75, 0.76, 0.78, 0.79, 0.8, 0.805, 0.81, 0.815, 0.82. The fitting curve is a stretched exponential $\propto\exp[-(t/\tau)^\beta]$ with $\beta=0.86$. Inset: fit of relaxation functions with the prediction of the mode coupling theory [Eq. (5)]. Densities $\rho=0.76$, 0.78, 0.79, 0.8, 0.805, 0.81, 0.815, 0.82.

$$\phi(t)=f+hc_\sigma g_\pm(t/t_\sigma), \tag{5}$$

with f (nonergodicity parameter) and h constants, $c_\sigma=|\sigma|^{1/2}$, $t_\sigma=|\sigma|^{-1/2a}$, and the separation parameter σ is negative in the liquid phase and positive in the glassy one. The transition can be driven by temperature, in which case $\sigma\propto T_c-T$, or by density, in which case $\sigma\propto\rho-\rho_c$. At short times, $t_0\ll t\ll t_\sigma$, the universal function has the asymptotic behavior $g_\pm(t/t_\sigma)\sim(t/t_\sigma)^{-a}$. At longer times, $t_\sigma\ll t\ll t_\alpha$, one has a functional form in the glassy phase, $g_+(t/t_\sigma)\sim(1-\lambda)^2$, and a distinct one in the liquid phase, $g_-(t/t_\sigma)\sim -B(t/t_\sigma)^b$. The parameters a, b are related as follows:

$$\frac{\Gamma^2(1-a)}{\Gamma(1-2a)}=\frac{\Gamma^2(1+b)}{\Gamma(1+2b)}=\lambda, \tag{6}$$

where λ is the so-called exponent parameter.

We have tried to fit the intermediate time scale of the correlation functions with the functional form of Eq. (5), as shown in Fig. 9 (inset). In agreement with the prediction of MCT the value of the exponent parameter λ, (and therefore of the exponents a, b) is constant within errors. The values extracted from the fit are: $\lambda=0.584\pm0.005$, $a=0.370\pm0.002$, $b=0.84\pm0.01$.

According to MCT, the exponent γ that characterizes the divergence of the relaxation times and of the inverse diffusivity should be the same, and equal to

$$\gamma=\frac{1}{2a}+\frac{1}{2b}. \tag{7}$$

As we said above, we found indeed that relaxation times and inverse diffusivity diverge with the same exponent $\gamma=3.53$. On the other hand, using the values of a and b obtained by the fits of the intermediate part of the relaxation functions, and using Eq. (7), one finds $\gamma=1.94\pm0.02$. This part of the prediction is therefore not verified.

For what concerns the long time regime ($t>t_\alpha$), the theory predicts that in the liquid phase, that is, for temperature $T>T_c$ or density $\rho<\rho_c$, the correlation functions decay

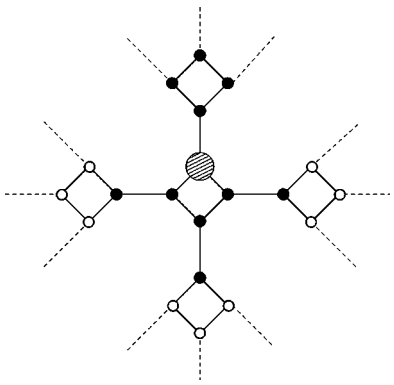

FIG. 10. The model of a treelike graph (here with $k=3$): each site is subdivided in $k+1$ positions (little circles), and connected to $k+1$ randomly chosen neighbors. A particle in a given position (big shaded circle) forbids the presence of another particle in the positions colored in black.

with a stretched exponential form, $c(t)\propto\exp[-(t/\tau_\alpha)^\beta]$, the exponent β being temperature (or density) independent. This prediction is called ''time-temperature superposition principle,'' but applies as well for density driven transitions.

In Fig. 9 we verify the prediction of MCT for densities between 0.75 and 0.81. In agreement with MCT the correlation functions collapse on the same stretched exponential when plotted versus t/τ_α. In the present case the value of the exponent is $\beta=0.86$.

IV. MEAN FIELD ANALYSIS

A. The random regular graph

In the past few years it came out that a special class of treelike random graphs, the ''random regular graph,'' is suitable to study the thermodynamics of complex and disordered systems in mean field [9,13,14]. The random regular graph is defined as a random graph with fixed connectivity $k+1$. In our case each site of the lattice is subdivided in $k+1$ internal position corresponding to the internal degree of freedom and each site is connected to $k+1$ sites randomly chosen. The hard-core interaction between nearest neighbor particles is showed in Fig. 10. For large number of sites N, such a graph locally looks like a portion of a Cayley tree, but it displays loops of length of order $\ln N$, where N is the total number of sites. Locally the problem is unfrustrated, but the presence of loops insures the existence of frustration which is a fundamental characteristic of glassy systems.

This particular treelike structure allows us to compute all the thermodynamic quantities (free energy, density, entropy, so forth) using an iterative method that, in the context of disordered systems, has been called the cavity method [15] and that in the liquid and in the crystalline phase reduces to the simple Bethe-Peierls iterative method. Let us consider a branch ending on a certain site i, connected to k sites $j\in\{1,\ldots,k\}$, and let $Z_0^{(i)}$, $Z_{ext}^{(i)}$, and $Z_{int}^{(i)}$ be the partition functions of the branch restricted to configurations in which the site i is empty, occupied in the ''external'' position and occupied in one of the k ''internal'' positions, respectively (see Fig. 11, where $k=3$). Now we can write the recursion

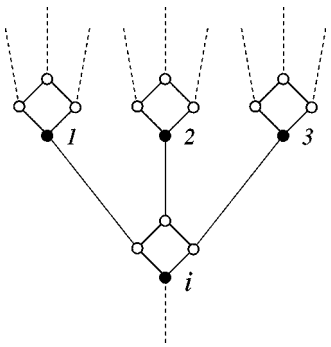

FIG. 11. Merging of the branches $j=1,\ldots,k$ (here with $k=3$) onto the site i: the ''external'' positions are those colored in black, the others are the ''internal'' ones.

relations between the partition functions of the branch ending on site i and the partition functions of the branches ending on sites j

$$Z_0^{(i)}=\prod_{j=1}^{k}(Z_0^{(j)}+Z_{ext}^{(j)}+Z_{int}^{(j)}), \tag{8a}$$

$$Z_{ext}^{(i)}=e^{\beta\mu}\prod_{j=1}^{k}(Z_0^{(j)}+Z_{int}^{(j)}), \tag{8b}$$

$$Z_{int}^{(i)}=e^{\beta\mu}\sum_{l=1}^{k}\left(\prod_{j\neq l}(Z_0^{(j)}+Z_{int}^{(j)})Z_0^{(l)}\right)$$

$$=e^{\beta\mu}\prod_{j=1}^{k}(Z_0^{(j)}+Z_{int}^{(j)})\left(\sum_{l=1}^{k}\frac{Z_0^{(l)}}{Z_0^{(l)}+Z_{int}^{(l)}}\right). \tag{8c}$$

It is convenient to introduce a couple of local cavity fields on each site, defined by the following relations: $e^{\beta h_i}=Z_{int}^{(i)}/Z_0^{(i)}$, $e^{\beta a_i}=(Z_{ext}^{(i)}+Z_{int}^{(i)})/Z_0^{(i)}$. The recursion relations for the local fields for the iteration process are

$$e^{\beta a_i}=e^{\beta\mu}\left(\prod_{j=1}^{k}\frac{1+e^{\beta h_j}}{1+e^{\beta a_j}}\right)\left(1+\sum_{j=1}^{k}\frac{1}{1+e^{\beta h_j}}\right), \tag{9a}$$

$$e^{\beta h_i}=e^{\beta\mu}\left(\prod_{j=1}^{k}\frac{1+e^{\beta h_j}}{1+e^{\beta a_j}}\right)\left(\sum_{j=1}^{k}\frac{1}{1+e^{\beta h_j}}\right), \tag{9b}$$

while the free energy shift in the merging process is given by

$$e^{-\beta\Delta F}=Z_0^{(i)}/\prod_{j=1}^{k}Z_0^{(j)}=\prod_{j=1}^{k}(1+e^{\beta a_j}). \tag{10}$$

To evaluate the total free energy density we have to compute the free energy shifts due to a site and link addition [13,14]

$$e^{-\beta\Delta F^{(1)}}=\prod_{j=1}^{k+1}(1+e^{\beta a_j})+e^{\beta\mu}\sum_{p=1}^{k+1}\prod_{j\neq p}(1+e^{\beta h_j}), \tag{11a}$$

$$e^{-\beta\Delta F^{(2)}}=1+e^{\beta a_1}+e^{\beta a_2}+e^{\beta(h_1+h_2)}. \tag{11b}$$

The total free energy will be then given by

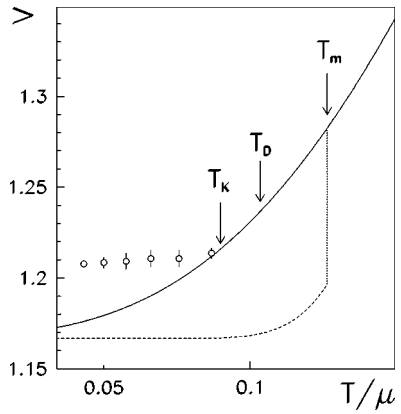

FIG. 12. Specific volume (inverse density) as a function of the temperature, on the random regular graph with $k=5$. Solid line: replica symmetric liquid phase; broken line: crystalline phase; open circles: glassy phase in the 1-step RSB approximation. Arrows mark the various temperatures cited in the text.

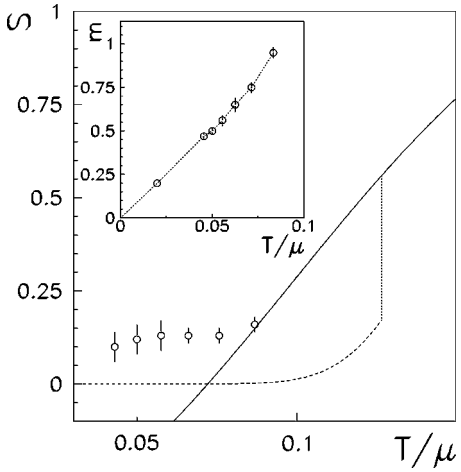

FIG. 13. Entropy per site as a function of the temperature, on the random regular graph with $k=5$. The notation is the same as in Fig. 12. Inset: parameter m as a function of the temperature. The line is a guide for the eye.

$$F=\Delta F^{(1)}-\frac{k+1}{2}\Delta F^{(2)}. \tag{12}$$

B. The replica symmetric solution

The replica symmetric solution (RS) of the problem corresponds to the case in which there is only one pure state and the local fields do not fluctuate from site to site ($h_i=h, a_i=a \forall i$). This homogeneous solution corresponds to the liquid phase characterized by translational invariance. This phase is expected to be stable for high values of the temperature T (or small values of the chemical potential μ).

In this case the local fields a and h are given by the fixed point of Eq. (9a). The free energy can be easily computed by Eq. (11a). From the local fields we can also evaluate the density ρ:

$$\rho=\frac{e^{\beta\mu}(k+1)(1+e^{\beta h})^k}{(1+e^{\beta a})^{k+1}+e^{\beta\mu}(k+1)(1+e^{\beta h})^k}. \tag{13}$$

Finally, since the internal energy per lattice site of the system is given by $E=-\mu\rho$, we obtain the following expression for the entropy per lattice site: $S=-\beta(F+\mu\rho)$.

As in the model studied by Biroli and Mézard [9], the entropy becomes negative for temperature below a certain value $T_{s=0}$. A similar behavior is observed for every $k>1$. This behavior indicates that the homogeneous solution is not appropriate to describe the high-density region. The key assumption of the RS approach is the absence of correlation between the various cavity sites or, equivalently, that the perturbation due to the variation of the local field on one cavity site remains localized and do not propagate in the whole lattice. This assumption is based on the consideration that the distance on the lattice between two generic sites is large for large N, and seems to work in the low-density region. It the high-density region it may fail because of the packing of the system in some disordered state.

It is also possible to find a crystalline (replica symmetric) solution of the problem where the fields do not fluctuate from site to site, but are different in different sites (breakdown of translational invariance). This is done via the introduction of three sublattices and three different couples of local fields. The merging is done taking into account the structure of the crystalline phase, described in Sec. II. The solution of the resulting equations appears discontinue at a spinodal point T_{sp}. It becomes thermodynamically stable when the corresponding free energy crosses the liquid one, at the melting temperature T_m. At that temperature we observe a first-order phase transition characterized by a spontaneous breakdown of the translational invariance, accompanied by a discontinuous change of the density and of the entropy per site. Increasing the chemical potential the density in the crystalline phase approaches quickly the maximum value $(k+1)/(k+2)$ and the entropy per site approaches quickly zero. For $k=5$ we find the following values for the spinodal and the melting temperature: $T_{sp}=0.1633\mu$ and $T_m=0.1444\mu$. The corresponding specific volume and entropy per site are shown as dashed lines in Figs. 12 and 13.

C. Replica symmetry breaking at the one step level

The liquid phase is metastable below T_m, describing a supercooled liquid. However, as we have seen, the predicted entropy per site becomes negative as the temperature is lowered, so this solution does not describe well the low temperature (high-density) region. In this region a great number of metastable glassy states appears, the system gets trapped in one of these states and falls out of equilibrium. The RS approach fails because it does not take into account the existence of several local minima of the free energy (pure states). We have then looked for a solution at the level of one-step replica symmetry breaking (RSB) [13–17].

In the high-density region many pure states exist and the local fields fluctuate also on the single site. To describe this situation we have to introduce a distribution probability $\mathcal{P}_i(a,h)$ defined as the probability that the fields a_i and h_i of the site i equal a and h.

In principle one should determine the number of metastable states for a given value of the free energy of the system. This function is called complexity, and the computation of its most appropriate form is a hard problem. In our cavity method formulation we assume the existence of many pure states but we do not consider the explicit form of the complexity. Roughly speaking, the cavity method assumes some properties about the correlations between two cavity sites and about the complexity in a system of N sites, and shows that these are self-consistently reproduced in a system with $N+1$ sites.

Because of the absence of quenched disorder we expect the glassy phase to be still translational invariant. Therefore we work in the so called ''factorized case'' in which the probability distribution of the local fields on the single site is the same for all the sites of the lattices. Using the cavity method in the one-step replica symmetry broken ansatz we obtain the following integral self-consistency equation for the probability distribution of the local fields

$$\mathcal{P}(a,h)=\mathcal{C}\int\prod_{j=1}^{k}[da_j dh_j \mathcal{P}(a_j,h_j)]\,\delta(a-a_i)\,\delta(h-h_i) \times\exp(-\beta m\Delta F), \tag{14}$$

where $\mathcal{C}$ is a normalization constant, a_i, h_i, and ΔF are functions of a_j and h_j via the recursion relations of Eqs. (9a) and (10), and the real parameter $m\in[0,1]$ is the usual one-step RSB parameter. The details of this calculation will be given in Sec. V.

The total free energy is now given by

$$F[m]=-\frac{1}{\beta m}\left\{\ln\int\prod_{j=1}^{k+1}da_j\,dh_j\,\mathcal{P}(a_j,h_j)e^{-\beta m\Delta F^{(1)}} -\frac{k+1}{2}\ln\int\prod_{j=1}^{2}da_j\,dh_j\,\mathcal{P}(a_j,h_j)e^{-\beta m\Delta F^{(2)}}\right\}, \tag{15}$$

where $\Delta F^{(1)}$ and $\Delta F^{(2)}$ depend on a_j and h_j via the Eq. (11a). The parameter m is fixed by the maximization of the free energy with respect to it. This is justified in the replica method since m turns out to be the breakpoint in Parisi's order parameter function at the one-step RSB level [15]. For a spin glass it has been rigorously proved [18] that in the $k\to\infty$ limit $F[m]$ is a lower bound to the correct free energy, so it is natural to find the preferred value of m by the maximization of $F[m]$.

It is interesting to note that the whole self-consistency procedure of Eq. (14) can be deduced in a variational formulation by the stability condition of the functional given in Eq. (15) with respect to changes of $\mathcal{P}(a,h)$.

D. Analytic solution at zero temperature

At $T=0$ Eq. (14) is easily solved. Indeed from Eq. (9a) in the $\beta\to\infty$ limit we note that the local fields on each site can only assume the following finite set of values:

$$a_i=(1-k)\mu,\ \ldots,0,\mu,$$

$$h_i=\begin{cases}a_i & \text{if } a_i<\mu\\ 0,\mu & \text{if } a_i=\mu.\end{cases} \tag{16}$$

The probability distribution of the local fields is then the sum of $k+2$ δ function $\mathcal{P}(a,h)=\sum_{r=1}^{k+2}p_r\delta(a-a_r)\,\delta(h-h_r)$. The self consistency Eq. (14) gives rise to $k+2$ algebraic equations for the weights of the δ functions p_r. For every value of $\beta m\mu$ we solve the equations for the coefficients. Finally we find that the maximum value of the free energy for $k=5$ is $F=-0.8265\mu$, obtained for $\beta m\mu=8.078$. Since $\beta m\mu$ stays finite for $\beta\to\infty$, m must go to zero at zero temperature, as it happens for the p-spin model.

E. Glassy solution at temperature $T>0$

At temperature $T>0$ we have solved Eq. (14) numerically with an iterative procedure and we have found a scenario identical to the one of p-spin models and discontinuous spin glasses.

We have discretized the distribution $\mathcal{P}(a,h)$ over a domain of the plane (a,h) using a fine grid spacing $da=dh=\mu/1024$. The starting distribution $\mathcal{P}(a,h)$ is the one that solves the equation at $T=0$ that we have previously described. We have slowly increased the temperature, and for each value of the temperature we have applied iteratively Eq. (14) until convergence. Before applying this procedure one must verify that the chosen domain covers the whole support of the distribution $\mathcal{P}(a,h)$.

In order to find the maximum of the free energy with respect to m it is useful to evaluate explicitly the derivative $dF[m]/dm$ [13]. For high values of the temperature we find that $\mathcal{P}(a,h)=\delta(a-\overline{a})\,\delta(h-\overline{h})$, where $\overline{a}$ and $\overline{h}$ are the values of the local fields in the liquid phase. Lowering the temperature we find first a dynamical transition at a certain temperature T_D, where a nontrivial solution of the 1-step RSB equation appears, signaling the existence of many pure states. This solution becomes thermodynamically stable below a static transition temperature T_s, where the maximum of the free energy as a function of m is at $m=1$. For $k=5$ we find that $T_D=0.105\mu$ and $T_s=0.087\mu$. The results for $k=5$ are shown in Figs. 12 and 13, and they are very similar to those found for other lattice glass models [9,19,20]. Fig. 13 shows also the behavior of the parameter m as a function of the temperature, which turns out to be very similar to the one found for the p-spin model. As the complexity (that is the logarithm of the number of metastable states) vanishes below T_s, the finite entropy below the static temperature must be interpreted as an ''intrastate'' entropy, due to the rattling of the particles inside the cages.

V. CONCLUSIONS

In conclusion, we have studied a lattice glass model with two body interactions. Monte Carlo simulations in three dimensions shows that the model, despite the presence of a crystalline state, has no tendency to crystallize. This feature allows the study of the supercooled regime without introduc-

ing a mixture, as in many models of glass. The model has a clear glassy behavior, and it is able to reproduce remarkably well the cage effect and the presence of two different time scales in the relaxation process.

A detailed analytical study in mean field on a random regular graph is presented. In this case, we find the scenario typical of *p*-spin glasses, recently reproduced by other models of glass. Further investigation is required to understand whether in finite dimensions the static transition observed in mean field is still present.

ACKNOWLEDGMENTS

This work was supported by MURST-PRIN-2003, INFM-PRA (HOP), and MIUR-FIRB 2002.

APPENDIX

In this section we report the details of the calculation of the self-consistency equation for the cavity method with the 1-step RSB ansatz [13,14]. The high-density region is characterized by the existence of many pure states. The number of pure states for a given value of the free energy is given by

$$\mathcal{N}(F) = \exp \Sigma(F). \tag{A1}$$

We assume that within a given pure state α the local fields a_i^α and h_i^α on different cavity sites are uncorrelated. Therefore the recursion Eq. (9a) continues to hold. However in this case we have to take into account the number of pure states at a given value of the free energy and the possibility of level crossings. We also assume $\Sigma(F)$ to be an extensive function.

Our aim is to find the self-consistency equation for the probability distribution of the local fields $\mathcal{P}(a,h)$. Let us consider a site i, connected to k cavity sites j. In each pure state α the local fields and the free energy shift are correlated, since they are both functions of the local fields in the neighbor sites in the state α a_j^α and h_j^α according to Eqs. (9a) and (10). However the triplets $(a_i^\alpha, h_i^\alpha, \Delta F_i^\alpha)$ are independent variables taken from a certain probability distribution that we will call $\mathcal{S}(a,h,\Delta F)$. Because of the recursion relations, this probability distribution has to verify the following iteration relation:

$$\mathcal{S}(a,h,\Delta F) = \int \prod_{j=1}^{k} [da_j\, dh_j\, \mathcal{P}(a_j,h_j)]\, \delta(a-a_i) \times \delta(h-h_i)\, \delta(\Delta F - \Delta F_i). \tag{A2}$$

In order to determine the probability distribution of the local fields $\mathcal{P}(a,h)$, we make the integration over all the possible free energy shifts. This leads to

$$\mathcal{P}(a,h) = \int d(\Delta F)\mathcal{S}(a,h,\Delta F)\mathcal{N}(F_N - \Delta F_N) = \int d(\Delta F)\mathcal{S}(a,h,\Delta F) \exp\left[N\Sigma\left(\frac{F_N - \Delta F_N}{N}\right)\right]. \tag{A3}$$

Since we are interested only on the local minima with the lowest free energy we can expand the exponential to the first order in $\Delta F = \Delta F_N / N$

$$\mathcal{P}(a,h) = \mathcal{C} \int d(\Delta F)\mathcal{S}(a,h,\Delta F) \exp(-\beta m \Delta F), \tag{A4}$$

where the parameter m is

$$m = \frac{1}{\beta}\frac{\partial \Sigma}{\partial f}. \tag{A5}$$

We can now make the integration over $d(\Delta F)$. The δ function selects only the right value of the free energy shift given in Eq. (10):

$$\mathcal{P}(a,h) = \mathcal{C} \int \prod_{j=1}^{k} [da_j\, dh_j\, \mathcal{P}(a_j,h_j)]\, \delta(a-a_i)\, \delta(h-h_i) \times \exp(-\beta m \Delta F_i). \tag{A6}$$

We have thus obtained the self-consistency Eq. (14).

The first-order expansion means that the number of pure states for a given value of the free energy is

$$\mathcal{N}(F) = \exp[m(F - F_{ref})], \tag{A7}$$

where F_{ref} is a reference free energy whose explicit value is completely irrelevant. This form of the density of states is the same found in the 1-step RSB formulation, where $m \in [0,1]$ is the usual 1-step RSB parameter. We finally conclude that our formulation is equivalent to the 1-step RSB ansatz.

In order to compute the free energy density we have to find the average values of the free energy shifts due to links and sites addition

$$e^{-\beta m \Delta F^{(1)}} = \int \prod_{j=1}^{k+1} [da_j\, dh_j\, \mathcal{P}(a_j,h_j)] \left(\prod_{j=1}^{k+1} (1 + e^{\beta a_j}) + e^{\beta \mu} \sum_{p=1}^{k+1} \prod_{j \neq p} (1 + e^{\beta h_j}) \right)^m,$$

$$e^{-\beta m \Delta F^{(2)}} = \int \prod_{j=1}^{2} [da_j\, dh_j\, \mathcal{P}(a_j,h_j)] (1 + e^{\beta a_1} + e^{\beta a_2} + e^{\beta(h_1+h_2)})^m. \tag{A8}$$

We have then derived the expression for the free energy density in the 1-step RSB given in Eq. (15).

[1] C.A. Angell, K.L. Ngai, G.B. McKenna, P.F. McMillan, and S.W. Martin, J. Appl. Phys. **88**, 3113 (2000).
[2] M.H. Choen and D.J. Turnbull, J. Chem. Phys. **31**, 1164 (1959).
[3] J.H. Gibbs and E.A. Di Marzio, J. Chem. Phys. **28**, 373 (1958); G. Adams, *ibid.* **43**, 139 (1965).
[4] P.G. Debenedetti and F.H. Stillinger, Nature (London) **410**, 259 (2001).
[5] F.H. Stillinger and T.A. Weber, Phys. Rev. A **25**, 978 (1982); S. Sastry, P.G. Debenedetti, and F.H. Stillinger, Nature (London) **393**, 554 (1998); F. Sciortino, W. Kob, and P. Tartaglia, Phys. Rev. Lett. **83**, 3214 (1999).
[6] W. Götze, in *Liquids, Freezing, and Glass Transition*, edited by J.P. Hansen, D. Levesque, and J. Zinn-Justin (Elsevier, Amsterdam, 1991).
[7] M. Mézard and G. Parisi, J. Chem. Phys. **111**, 1076 (1999); M. Mézard, in *More is Different*, edited by M.P. Ong and R.N. Bhatt (Princeton University Press, Princeton, NJ, 2001).
[8] T.R. Kirkpatrick and D. Thirumalai, Phys. Rev. Lett. **58**, 2091 (1987).
[9] G. Biroli and M. Mézard, Phys. Rev. Lett. **88**, 025501 (2002).
[10] A. Lawlor, D. Reagan, G.D. McCullagh, P. De Gregorio, P. Tartaglia, and K.A. Dawson, Phys. Rev. Lett. **89**, 245503 (2003).
[11] M. Pica Ciamarra, M. Tarzia, A. de Candia, and A. Coniglio, Phys. Rev. E **67**, 057105 (2003).
[12] R. Di Leonardo, L. Angelani, G. Parisi, and G. Ruocco, Phys. Rev. Lett. **84**, 6054 (2000).
[13] M. Mézard and G. Parisi, Eur. Phys. J. B **20**, 217 (2001).
[14] M. Mézard and G. Parisi, J. Stat. Phys. **111**, 1 (2003).
[15] M. Mézard, G. Parisi, and M.A. Virasoro, *Spin Glass Theory and Beyond* (World Scientific, Singapore, 1987).
[16] R. Monasson, J. Phys. A **31**, 513 (1998).
[17] Y.Y. Goldschmidt and P.Y. Lai, J. Phys. A **23**, L775 (1990).
[18] F. Guerra, Commun. Math. Phys. **233**, 1 (2003).
[19] S. Franz, M. Leone, F. Ricci-Tersenghi, and R. Zecchina, Phys. Rev. Lett. **87**, 127209 (2001).
[20] L. Hartmann and M. Weigt, Europhys. Lett. **62**, 533 (2003).